The Astrophysical Journal Letters, 899:L20 (6pp), 2020 August 10 https://doi.org/10.3847/2041-8213/abaaaa

Discovery of the Black Hole X-Ray Binary Transient MAXI J1348–630

Mayu Tominaga[1], Satoshi Nakahira[1], Megumi Shidatsu[2], Motoki Oeda[3], Ken Ebisawa[1], Yasuharu Sugawara[1], Hitoshi Negoro[4], Nobuyuki Kawai[3], Mutsumi Sugizaki[5], Yoshihiro Ueda[6], and Tatehiro Mihara[7]
[1] Institute of Space and Astronautical Science (ISAS), Japan Aerospace Exploration Agency (JAXA), 3-1-1 Yoshinodai, Chuo, Sagamihara, Kanagawa, 252-5210, Japan; tominaga@ac.jaxa.jp
[2] Department of Physics, Ehime University, 2-5, Bunkyocho, Matsuyama, Ehime 790-8577, Japan
[3] Department of Physics, Tokyo Institute of Technology, 2-12-1 Ookayama, Meguro-ku, Tokyo 152-8551, Japan
[4] Department of Physics, Nihon University, 1-8-14 Kanda-Surugadai, Chiyoda-ku, Tokyo 101-8308, Japan
[5] National Astronomical Observatories, Chinese Academy of Sciences, 20A Datun Road, Beijing 100012, People's Republic of China
[6] Department of Astronomy, Kyoto University, Kitashirakawa-Oiwake-cho, Sakyo-ku, Kyoto 606-8502, Japan
[7] High Energy Astrophysics Laboratory, RIKEN, 2-1 Hirosawa, Wako, Saitama 351-0198, Japan
Received 2020 April 7; revised 2020 July 22; accepted 2020 July 30; published 2020 August 13

Abstract

We report the first half-year monitoring of the new Galactic black hole candidate MAXI J1348–630, discovered on 2019 January 26 with the Gas Slit Camera on board the Monitor of All-sky X-ray Image (MAXI). During the monitoring period, the source exhibited two outburst peaks, where the first peak flux (at $T = 14$ days from the discovery of $T = 0$) was ∼4 Crab (2–20 keV) and the second one (at $T = 132$ days) was ∼0.4 Crab (2–20 keV). The source exhibited distinct spectral transitions between the high/soft and low/hard states and an apparent "q"-shape curve on the hardness-intensity diagram, both of which are well-known characteristics of black hole binaries (BHBs). Compared to other bright black hole transients, MAXI J1348–630 is characterized by its low disk temperature (∼0.75 keV at the maximum) and high peak flux in the high/soft state. The low peak temperature leads to a large innermost radius that is identified as the innermost stable circular orbit, determined by the black hole mass and spin. Assuming the empirical relation between the soft-to-hard transition luminosity ($L_{\rm trans}$) and the Eddington luminosity ($L_{\rm Edd}$), $L_{\rm trans}/L_{\rm Edd} \approx 0.02$, and a face-on disk around a non-spinning black hole, the source distance and the black hole mass are estimated to be $D \approx 4$ kpc and $\sim 7(D/4\ {\rm kpc})M_{\odot}$, respectively. The black hole is more massive if the disk is inclined and the black hole is spinning. These results suggest that MAXI J1348–630 may host a relatively massive black hole among the known BHBs in our Galaxy.

Unified Astronomy Thesaurus concepts: Black holes (162); Compact objects (288); High energy astrophysics (739); X-ray novae (1818); Stellar accretion disks (1579)

1. Introduction

Black hole binaries (BHBs), those consisting of a stellar mass black hole and a main-sequence star, are known to exhibit two distinct X-ray spectral states; the "low/hard" state and the "high/soft" state (e.g., Remillard & McClintock 2006; Belloni 2009; McClintock & Remillard 2009). The low/hard state is observed when the mass accretion rate is relatively low, where the optically thick/geometry-thin standard disk is likely to be truncated before reaching the innermost stable circular orbit (ISCO), and the inner disk becomes a radiatively inefficient hot accretion flow. When the accretion rate becomes higher than a certain threshold, the inner disk switches its nature from the optically thin/geometrically thick state to the standard disk, where the innermost radius will reach to the ISCO.

One of the most efficient ways to discover such BHBs and study their state transitions is to continuously monitor the entire sky in X-rays, because most BHBs are transients and exhibit unpredictable X-ray outbursts. The Monitor of All-sky X-ray Image (MAXI; Matsuoka et al. 2009), which is operated on the International Space Station (ISS) and is surveying ∼85% of the sky every ∼92 minutes (corresponding to the ISS orbital period, where each strip of the sky is exposed for a duration of 40–100 s), is an ideal instruments for that purpose. In fact, since 2009, MAXI has discovered 13 new BHB transients and monitored their state transitions extensively (Negoro 2019; Negoro et al. 2019b).

In this Letter, we report the discovery of MAXI J1348−630 on 2019 January 26 by MAXI (Yatabe et al. 2019) and the results of continuous monitoring of the source until 2019 August 3 (176 days after the discovery) including two outbursts (see also Jana et al. 2020 for the first outburst). Since its discovery, the source was subsequently observed with other X-ray telescopes, Swift/X-ray Telescope (Kennea & Negoro 2019), the INTErnational Gamma-Ray Astrophysics Laboratory (INTEGRAL; Lepingwell et al. 2019), and the Neutron star Interior Composition Explorer (NICER; Sanna et al. 2019). We also analyze Swift data to supplement the energy bands above ∼15 keV and below ∼2.0 keV, where MAXI is not sensitive.

An optical counterpart was detected by iTelescope.Net T31 0.51 m telescope in Siding Spring (Denisenko et al. 2019), Swift/UltraViolet and Optical Telescope (UVOT; Kennea & Negoro 2019), and Las Cumbres Observatory network 2 and 1 m telescopes (Russell et al. 2019b). The radio counterpart was detected by Australia Telescope Compact Array (ATCA; Russell et al. 2019c) with a flat spectrum consistent with a compact jet.

2. Observation and Data Reduction

2.1. MAXI

MAXI J1348−630 was detected with the Gas Slit Camera (GSC; Mihara et al. 2011; Sugizaki et al. 2011) through the MAXI nova alert system (Negoro et al. 2016) at 03:16 UT on

2019 January 26 (MJD 58509, $T = 0$; hereafter, T is defined as MJD-58509), where the X-ray flux was 47 ± 8 mCrab (4–10 keV; Yatabe et al. 2019). We analyzed the long-term data of MAXI J1348–630 from the discovery to 2019 August 3 using the MAXI/GSC on-demand web interface[8] (Nakahira et al. 2013). The source events were extracted within a circular region of 2.°1 radius around the source position (R.A., decl.) = (207.°053, −63.274; Kennea & Negoro 2019). The background region was set to a concentric ring with the outer radius of 3.°0. We used only the GSC counters with minimum damages, GSC #2 and #7 operated at the high voltage of 1550 V, and #4 and #5 at 1660 V.

2.2. Swift

The Burst Alert Telescope (BAT) on board Swift searches all-sky for gamma-ray bursts, and also provides light curves of major sources in 15–50 keV. We used the public BAT light curves available on the BAT Transition Monitor website (Krimm et al. 2013).[9] We also used the pointing observation data of the X-Ray Telescope (XRT; Burrows et al. 2005). We used the on-demand web interface (Evans et al. 2009)[10] to reduce the XRT data, which has observation IDs of 00011107024, 00011107029, and 0001110702. In the spectral analysis, we adopted the response matrix file `swxwt0to2s6_20131212v015.rmf` provided via the High Energy Astrophysics Science Archive Research Center (HEASARC) calibration database.[11]

3. Results

3.1. MAXI/GSC

Figure 1 shows the X-ray light curves of MAXI J1348−630 in 2–6 keV (soft) and 6–20 keV (hard) bands, and their hardness ratio, as well as the light curve in 15–50 keV obtained with Swift/BAT. Because the Crew Dragon Spacecraft launched by SpaceX was located on the line of sight during $T = 36$–41, we do not use the data during this period.

After the discovery on 2019 January 26 (MJD 58509, $T = 0$), the hard band flux rapidly increased and reached the peak on $T = 8$. The source spectra showed a distinct hard-to-soft transition between $T = 8$ and $T = 21$ (Bassi et al. 2019; Cangemi et al. 2019; Nakahira et al. 2019). The source was initially in the hard state, where the hardness ratio was almost constant at around 0.5 until the hard band peak ($T = 8$). After that, the hard band flux rapidly dropped until $T \sim 21$, then slowly declined throughout the following 70 days. On the other hand, the soft band flux further increased after the hard band peak, then reached its peak on February 9 ($T = 14$) at $\sim 1.1 \times 10^1$ photons cm^{-2} s^{-1} (2–6 keV). The flux observed with MAXI/GSC (2–20 keV) declined steadily during $T = 21$–91 by keeping the constant hardness ratio at around 0.05. Near the end of the first outburst ($T = 91$–95), the source went back to the hard state with the hardness ratio ∼0.5. After $T = 95$, the source gradually faded, and finally reached below the detection limit of MAXI/GSC at $T = 104$.

On 2019 May 31 (MJD 58634, $T = 126$), the source brightened again and reached the peak flux ∼1.0 photons cm^{-2} s^{-1} (2–20 keV) on $T = 132$ (Negoro et al. 2019a; Russell et al. 2019a), which is about 10% of the first peak, followed by steady decline. The hardness ratio during the re-brightening phase was almost constant at 0.5, thus the source was in the hard state throughout the second outburst. After $T = 175$, the source got down below the detection limit again.

The hardness-intensity diagram (HID) in Figure 2 shows a clear "q"-curve (e.g., Nakahira et al. 2019). According to the time history of the hardness ratio, we classified the entire observation period into the three spectral states; the low/hard state of $T = 0$–8 and 107–191, the transition state of $T = 8$–21 and 91–106, and the high/soft state of $T = 21$–91.

Both the distinct spectral transitions and the "q"-shaped HID are common properties of BHBs (e.g., Homan & Belloni 2005). Therefore, we fitted the observed spectra with a standard BHB spectral model. We used `xspec` version 12.10.0c for spectral model fitting. Because daily MAXI/GSC data do not have enough photon statistics for model fitting, we adaptively accumulated data for several days using the Bayesian block representations with the normalization constant $p_0 = 0.5$ (Scargle et al. 2013). In the high/soft state, we adopt the optically thick Multi-Color-Disk blackbody model `diskbb` (Mitsuda et al. 1984) and its inverse-Compton scattering approximated by `simpl` (Steiner et al. 2009). We applied the interstellar absorption of Tuebingen-Boulder model `tbabs` with the Solar abundance given by Wilms et al. (2000). We fixed the neutral hydrogen column density at $N_{\rm H} = 8.6 \times 10^{21}$ cm^{-2} obtained from Swift/XRT data (see Section 3.2). The model is described as `tbabs * simpl * diskbb` where free parameters are scattering fraction ($F_{\rm scat}$) of `simpl`, innermost temperature ($T_{\rm in}$) and normalization ($N_{\rm disk}$) of `diskbb`. The photon index (Γ) is assumed to be constant at the canonical value $\Gamma = 2.5$ because the hard tail in the high/soft state is so weak that the index is hardly constrained (e.g., McClintock & Remillard 2009). Here, we confirmed that the disk temperature $T_{\rm in}$ is only slightly increased or decreased by ∼0.03 keV when Γ is changed to 2.0 or 3.0 even when the hard tail was the strongest ($T = 23$). In the low/hard state, the model is described by `tbabs * powerlaw` where free parameters are photon index (Γ) and normalization of `powerlaw`. In the transition states, we applied the same model as in the high/soft state, but Γ was treated as a free parameter. After the phenomenological spectral fittings, we estimate a more realistic innermost disk radius $R_{\rm in}$ as follows. Definition of the `diskbb` normalization $N_{\rm disk}$ is

$$N_{\rm disk} = \left(\frac{r_{\rm in}}{D/10\ {\rm kpc}} \right)^2 \cos i \qquad (1)$$

where D is the source distance, i is the disk inclination angle, and $r_{\rm in}$ is an apparent disk radius. We estimate $R_{\rm in}$ as

$$R_{\rm in} = \xi \kappa^2 r_{\rm in} \qquad (2)$$

where $\xi = 0.41$ is a correction factor for the inner boundary condition (Kubota et al. 1998), $\kappa = 1.7$ is the color hardening factor (Shimura & Takahara 1995). Figure 3 shows a time history of the spectral fitting parameters (with errors of 90% confidence limits of statistical uncertainties), where $R_{\rm in}$ is calculated assuming the most plausible distance $D = 4$ kpc (see the Discussion below) and $i = 0$. Figure 4 shows the results of model fittings on several key dates.

[8] http://maxi.riken.jp/mxondem
[9] https://swift.gsfc.nasa.gov/results/transients/
[10] https://www.swift.ac.uk/user_objects/
[11] https://heasarc.gsfc.nasa.gov/FTP/caldb/data/swift/xrt/cpf/rmf/

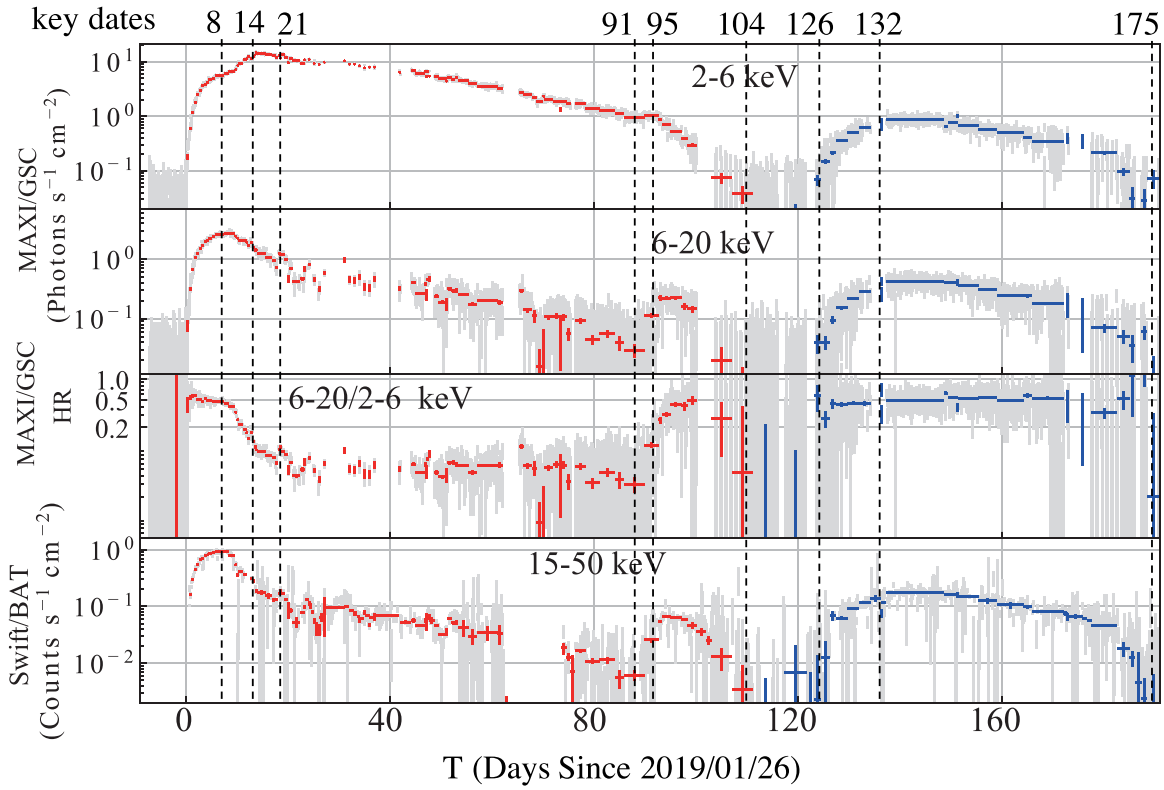

Figure 1. MAXI/GSC 2–6 and 6–20 keV light curves, hardness ratio between the two energy bands, and the 15–50 keV Swift/BAT light curve, from top to bottom. Gray points indicate individual scans and colored points are adaptively binned data (see the text). The difference in color represents the first outburst (red) and the second one (blue). Black dashed lines indicate the following key dates; $T = 8$ (hard band peak), $T = 14$ (soft band peak), $T = 21$ (end of the hard–soft transition), $T = 91$ (start of soft–hard transition), $T = 95$ (end of the soft–hard transition), $T = 104$ (disappearance), $T = 126$ (reappearance), $T = 132$ (peak after the reappearance), and $T = 175$ (second disappearance).

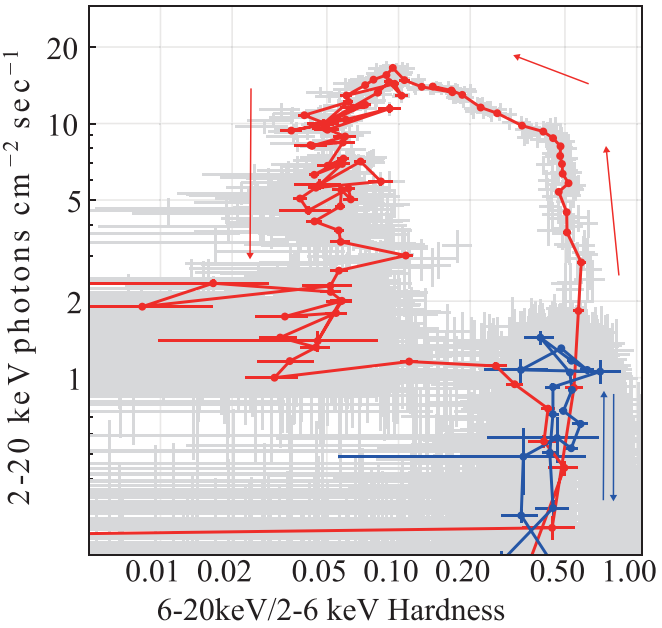

Figure 2. Hardness-intensity diagram (HID) of the hardness ratio (6–20 keV/2–6 keV) vs. 2–20 keV intensity. The gray points and the color points connected by line are produced in the same manner as in Figure 1. Arrows indicate the directions along with dates.

3.2. *Swift/XRT*

Because the MAXI/GSC data with the energy band above 2 keV cannot precisely determine $N_{\rm H}$ of the interstellar absorption, we analyzed the data obtained with Swift/XRT, which is more sensitive in the lower energy range (1–10 keV). We chose the data of $T = 56$, 65, and 85 in the high/soft state, and fitted these spectra with the same spectral model. The obtained $N_{\rm H}$ value was $\sim 8.6 \times 10^{21}$ cm^{-2} at $T = 85$, which we adopt throughout this Letter, and those values in the other dates were agreed within $\sim 2.0 \times 10^{21}$ cm^{-2}.

We also conducted joint spectral fitting of Swift/XRT and MAXI/GSC data taken on $T = 56$, 65, and 85. The result of $T = 85$ is shown in the bottom-middle panel of Figure 4. When $T_{\rm in}$ was independently fitted to each instrument, MAXI GSC gave 0.46 keV, and Swift/XRT gave 0.52 keV. We found that Swift/XRT always gave slightly higher $T_{\rm in}$ values than MAXI/GSC during the high/soft state. This is probably due to the presence of a significant hard tail, which is hardly constrained by Swift/XRT below $\sim$7 keV but clearly recognized by MAXI.

4. Discussion

We discuss the nature of the new X-ray transient MAXI J1348–630 from the results of the data analysis presented above. The source exhibited clear spectral transitions (Figure 1) and a q-shaped track on the HID (Figure 2), both of which are well-known characteristics of BHBs. Furthermore, we successfully fitted energy spectra in the three spectral states with their typical spectral models. (Figure 3). These facts strongly suggest that MAXI J1348–630 is a new BHB.

Here, we point out that the maximum disk temperature is as low as $T_{\rm in} \approx 0.75$ keV even at the high/soft state luminosity

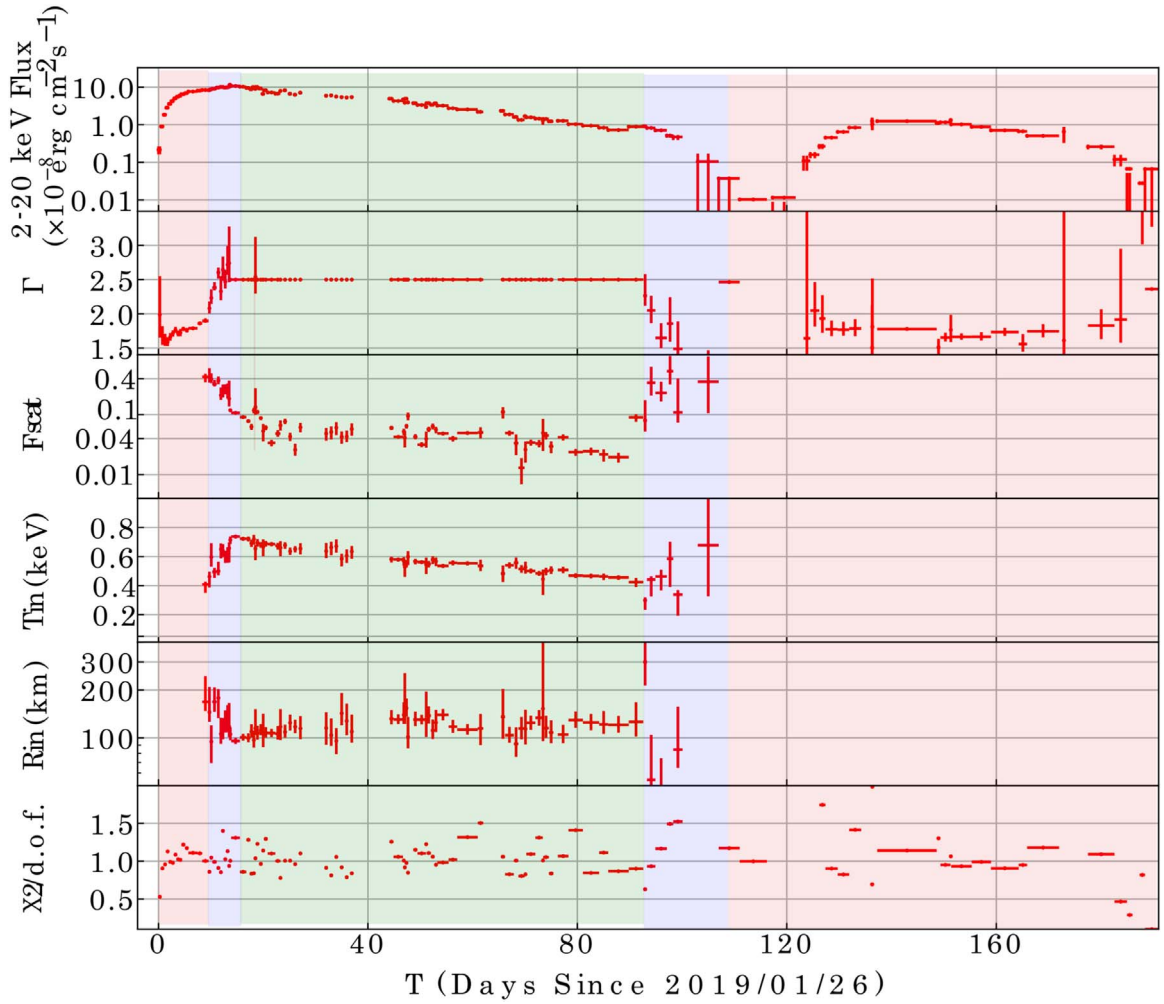

Figure 3. Time evolution of the spectral parameters derived from model fits to the 2–20 keV MAXI/GSC spectra (90% confidence). $R_{\rm in}$ is calculated assuming $D = 4$ kpc and $i = 0$ (face-on geometry). The background colors represent the spectral states; low/hard state (red; $T = 0$–8 and 107–191), transition state (blue; $T = 8$–21 and 91–106), and high/soft state (green; $T = 21$–91). According to the spectral states, fitting models are different (see the text for details).

peak ($T = 14$). This is remarkably lower compared to other luminous black hole transients, where the maximum disk temperature almost always exceeds ∼1 keV. The low disk temperature and the high luminosity lead to the large innermost radius because the disk luminosity is proportional to $R_{\rm in}^2\, T_{\rm in}^4$. The large innermost radius suggests that MAXI J1348–630 harbors a relatively massive black hole compared to other black holes.

In particular, the innermost radius of the accretion disk ($R_{\rm in}$) is nearly constant during the high/soft state, while the 2–20 keV flux and the disk temperature were significantly variable (Figure 3). This is a remarkable property in the high/soft-state BHBs, such that the constant radius corresponds to the ISCO (e.g., Tanaka 1989; Ebisawa et al. 1993; Steiner et al. 2010), which is determined by black hole mass and spin. In the case of non-rotating black holes, ISCO is equal to three times the Schwarzschild radius. Thus, from the average innermost radius of the disk, $R_{\rm in} \approx 114 \pm 14\ (D/4\ {\rm kpc})(\cos i)^{-1/2}$ km, the black hole mass $M_{\rm BH}$ is estimated to be

$$M_{\rm BH} = \frac{c^2 R_{\rm in}}{6G} \approx 13 \pm 2 \left(\frac{D}{4\ {\rm kpc}}\right)(\cos i)^{-\frac{1}{2}} M_\odot. \quad (3)$$

The expected distance–mass relation in $i = 0°$ and 60° are shown in Figure 5.

In addition, BHBs are known to show similar luminosity dependence of the spectral states. For instance, in the current case of MAXI J1348–630, the flux at the soft-to-hard transition ($T = 91$) is ∼10% of the peak flux in the high/soft state ($T = 14$); this value is consistent with those of other BHBs discovered by MAXI, such as MAXI J1820+070 (∼12%; Shidatsu et al. 2019) and MAXI J1910−057 (∼10%–15%; Nakahira et al. 2014). Furthermore, it was pointed out that the soft-to-hard transition typically occurs at 1%–4% of the Eddington luminosity ($L_{\rm Edd}$; Maccarone 2003). Namely, the bolometric luminosity soon after the soft-to-hard transition is expected to be 0.01–0.04 $L_{\rm Edd}$. The gray curves in Figure 5 give the distance–mass relation of $L_{\rm trans}/L_{\rm Edd} = 0.01$ and 0.04, where we employed the bolometric flux at the soft-to-hard transition $\sim 1.7 \times 10^{-8}$ erg s^{-1} cm^{-2} on $T = 96$ and $L_{\rm Edd} = 1.3 \times 10^{38}\ (M/M_\odot)$ erg s^{-1}.

Next, we try to constrain the source distance. The galactic coordinate of the source is $(l,\ b) = (309.3,\ -1.1)$, which is tangential to the Galactic Scutum–Centaurus arm. If MAXI J1348−630 locates in the Scutum–Centaurus arm, the distance is estimated to be ∼4–8 kpc (e.g., Xu et al. 2018). However, the value of $N_{\rm H} = 8.6 \times 10^{21}$ cm^{-2} implies that the source is

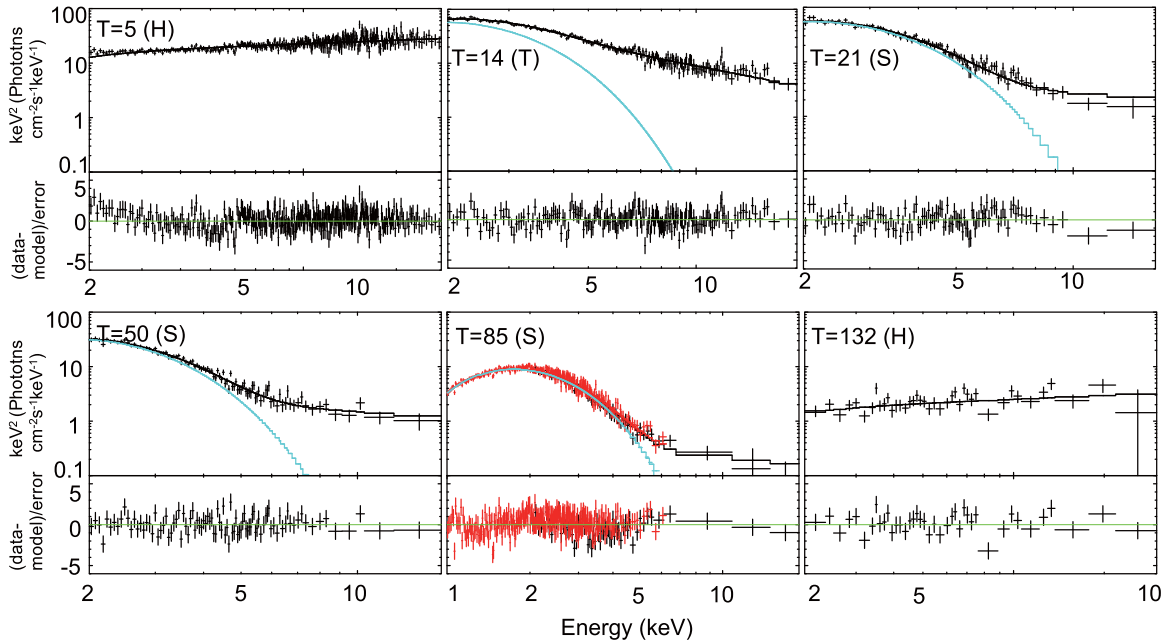

Figure 4. Results of spectral fittings on $T = 5$, 14, 21, 50, 85, and 132. The letters H, T, and S in the brackets represent the hard (low) state, transition state, and soft (high) state, respectively. The spectra on $T = 85$ shows the joint fit of Swift/XRT (red lines) and MAXI/GSC (black lines). For the transition and high/soft state spectra, we plotted the original `diskbb` spectra (cyan lines) without being Compton upscattering ($F_{\rm scat} = 0$) in order to demonstrate the effect of Comptonization.

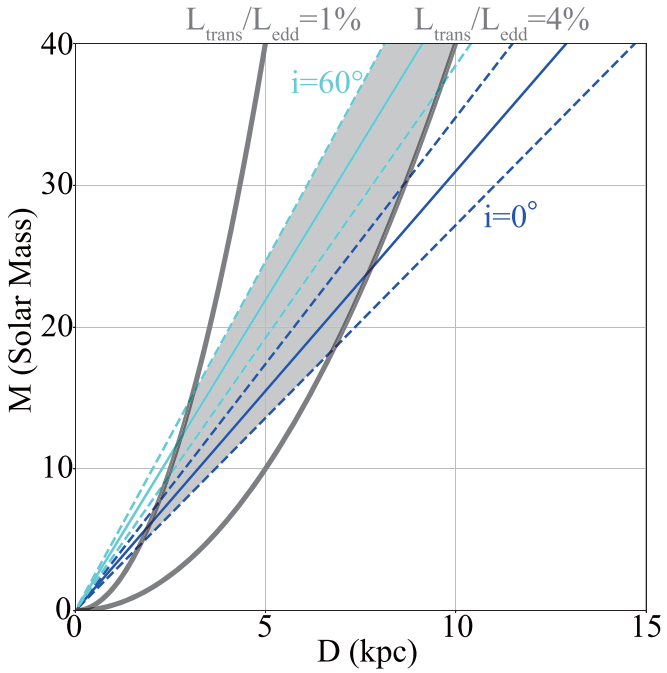

Figure 5. Observational constrains on the distance–mass diagram. The two solid colored lines represent Equation (3) when $i = 0°$ (blue) and 60° (cyan). The dashed lines with the same colors denote the error region due to systematic error. The gray curves give the empirical relation that the luminosity after the soft-to-hard transition ($T = 96$) is 0.01–0.04 $L_{\rm Edd}$. The shaded region represents the plausible mass and distance range.

located in front of the arm at ∼3–4 kpc. If we adopt the most likely index $L_{\rm trans}/L_{\rm Edd} \approx 0.02$ (Vahdat Motlagh et al. 2019), the distance becomes ∼3.8 kpc for the face-on disk. It is consistent with the estimates from optical observations (Charles et al. 2019; Russell et al. 2019b).

In order to estimate the black hole mass more precisely, taking account of the relativistic effects, we tried the `kerrbb` model instead of the `diskbb` model (Li et al. 2005). The `kerrbb` model gives relations among the spinning parameter a, inclination angle i, and black hole mass M under a given source distance, mass accretion rate, and spectral hardening factor (κ in Equation (2)). We carried out a joint fit to the MAXI/GSC and Swift/XRT spectra at $T = 85$ fixing $D = 4$ kpc and $\kappa = 1.7$ for several discrete a and i values, only allowing the black hole mass and mass accretion rate to be free. Consequently, the values of $M/M_\odot$ were 7.0 ($a = 0$, $i = 0°$), 14 ($a = 0$, $i = 60°$), 18 ($a = 0.998$, $i = 0°$), and 76 ($a = 0.998$, $i = 60°$). Hence, we have reached a robust conclusion that MAX J1348–630 hosts a relatively massive black hole. Jana et al. (2020) also suggest a black hole mass of $\sim 9\,M_\odot$ based on an independent accretion disk spectral model.

The binarity of MAXI J1348–63 has never been confirmed from observations of the dynamical motion. Follow-up detailed optical/infrared spectroscopic observations are strongly encouraged to constrain the black hole mass as well as the source distance more precisely.

This research has made use of the MAXI data provided by RIKEN, JAXA, and the MAXI team, and the Swift data and analysis software provided by HEASARC, which is a service of the Astrophysics Science Division at NASA/GSFC.

ORCID iDs

Mayu Tominaga https://orcid.org/0000-0002-1163-6077
Satoshi Nakahira https://orcid.org/0000-0001-9307-046X
Megumi Shidatsu https://orcid.org/0000-0001-8195-6546
Ken Ebisawa https://orcid.org/0000-0002-5352-7178
Yasuharu Sugawara https://orcid.org/0000-0001-6749-1199
Nobuyuki Kawai https://orcid.org/0000-0001-9656-0261
Mutsumi Sugizaki https://orcid.org/0000-0002-1190-0720
Yoshihiro Ueda https://orcid.org/0000-0001-7821-6715
Tatehiro Mihara https://orcid.org/0000-0002-6337-7943

References

Bassi, T., del Santo, M., D'Ai, A., et al. 2019, ATel, 12477, 1
Belloni, T. M. 2009, LNP, 794, 53
Burrows, D. N., Hill, J. E., Nousek, J. A., et al. 2005, SSRv, 120, 165
Cangemi, F., Belloni, T., & Rodriguez, J. 2019, ATel, 12471, 1
Charles, P. A., Buckley, D. A. H., Kotze, E., et al. 2019, ATel, 12480, 1
Denisenko, D., Denisenko, I., Evtushenko, M., et al. 2019, ATel, 12430, 1
Ebisawa, K., Makino, F., Mitsuda, K., et al. 1993, ApJ, 403, 684
Evans, P. A., Beardmore, A. P., Page, K. L., et al. 2009, MNRAS, 397, 1177
Homan, J., & Belloni, T. 2005, Ap&SS, 300, 107
Jana, A., Debnath, D., Chatterjee, D., et al. 2020, ApJ, 897, 13
Kennea, J. A., & Negoro, H. 2019, ATel, 12434, 1
Krimm, H. A., Holland, S. T., Corbet, R. H. D., et al. 2013, ApJS, 209, 14
Kubota, A., Tanaka, Y., Makishima, K., et al. 1998, PASJ, 50, 667
Lepingwell, A. V., Fiocchi, M., Bird, A. J., et al. 2019, ATel, 12441, 1
Li, L.-X., Zimmerman, E. R., Narayan, R., & McClintock, J. E. 2005, ApJS, 157, 335
Maccarone, T. J. 2003, A&A, 409, 697
Matsuoka, M., Kawasaki, K., Ueno, S., et al. 2009, PASJ, 61, 999
McClintock, J. E., & Remillard, R. A. 2009, Compact Stellar X-ray Sources (Cambridge: Cambridge Univ. Press), 157
Mihara, T., Nakajima, M., Sugizaki, M., et al. 2011, PASJ, 63, S623
Mitsuda, K., Inoue, H., Koyama, K., et al. 1984, PASJ, 36, 741
Nakahira, S., Ebisawa, K., Negoro, H., et al. 2013, Journal of Space Science Informatics, 2, 29, http://id.nii.ac.jp/1696/00001986
Nakahira, S., Kawai, N., Negoro, H., et al. 2019, ATel, 12469, 1
Nakahira, S., Negoro, H., Shidatsu, M., et al. 2014, PASJ, 66, 84
Negoro, H. 2019, AstHe, 112, 627, http://www.asj.or.jp/geppou/archive_open/2019_112_09/112-9_627.pdf
Negoro, H., Kohama, M., Serino, M., et al. 2016, PASJ, 68, S1
Negoro, H., Mihara, T., Nakajima, M., et al. 2019a, ATel, 12838, 1
Negoro, H., Miike, K., Nakajima, M., et al. 2019b, ATel, 13256, 1
Remillard, R. A., & McClintock, J. E. 2006, ARA&A, 44, 49
Russell, D. M., Al Yazeedi, A., Bramich, D. M., Baglio, M. C., & Lewis, F. 2019a, ATel, 12829, 1
Russell, D. M., Baglio, C. M., & Lewis, F. 2019b, ATel, 12439, 1
Russell, T., Anderson, G., Miller-Jones, J., et al. 2019c, ATel, 12456, 1
Sanna, A., Uttley, P., Altamirano, D., et al. 2019, ATel, 12447, 1
Scargle, J. D., Norris, J. P., Jackson, B., & Chiang, J. 2013, ApJ, 764, 167
Shidatsu, M., Nakahira, S., Murata, K. L., et al. 2019, ApJ, 874, 183
Shimura, T., & Takahara, F. 1995, ApJ, 445, 780
Steiner, J. F., McClintock, J. E., Remillard, R. A., et al. 2010, ApJL, 718, L117
Steiner, J. F., Narayan, R., McClintock, J. E., & Ebisawa, K. 2009, PASP, 121, 1279
Sugizaki, M., Mihara, T., Serino, M., et al. 2011, PASJ, 63, S635
Tanaka, Y. 1989, in ESA Special Publication, Vol. 1, Two Topics in X-Ray Astronomy, Volume 1: X Ray Binaries. Volume 2: AGN and the X Ray Background, ed. J. Hunt & B. Battrick (Noordwijk: ESA), 3
Vahdat Motlagh, A., Kalemci, E., & Maccarone, T. J. 2019, MNRAS, 485, 2744
Wilms, J., Allen, A., & McCray, R. 2000, ApJ, 542, 914
Xu, Y., Hou, L.-G., & Wu, Y.-W. 2018, RAA, 18, 146
Yatabe, F., Negoro, H., Nakajima, M., et al. 2019, ATel, 12425, 1